

# White-light emission from $\text{Y}_2\text{SiO}_5\text{:Ce}^{3+}$ , $\text{Tb}^{3+}$ and $\text{Sr}_2\text{Si}_5\text{N}_8\text{:Eu}^{2+}$ phosphor blends: a predictive model

Dora-Luz Flores<sup>1</sup> ✉, Everardo Gutierrez<sup>1</sup>, David Cervantes<sup>1</sup>, Marco Chacon<sup>1</sup>, Gustavo Hirata<sup>2</sup>

<sup>1</sup>Universidad Autónoma de Baja California, Carretera Transpeninsular Ensenada-Tijuana 3917 Colonia Playitas, Ensenada, B.C., C.P. 22860 Mexico

<sup>2</sup>Centro de Nanociencias y Nanotecnología – UNAM, Mexico

✉ E-mail: dflores@uabc.edu.mx

Published in Micro & Nano Letters; Received on 7th March 2017; Accepted on 15th March 2017

In recent years, there has been an increasing interest in developing multifunctional materials that can be used in different areas, such as artificial lighting. White light-emitting diodes offer the possibility of efficient, safe, and reliable solid-state lighting. This study presents a synthesis and characterisation process of a white-light emitting phosphor based on the combination of rare earth-activated  $\text{Y}_2\text{SiO}_5\text{:Ce}^{3+}$ ,  $\text{Tb}^{3+}$  (YSO) and  $\text{Sr}_2\text{Si}_5\text{N}_8\text{:Eu}^{2+}$  (SSN) phosphors. The YSO phosphor was prepared by combustion synthesis, whereas the SSN phosphor was prepared by solid-state reaction under  $\text{N}_2/\text{H}_2$  atmosphere. Photoluminescence measurements showed the contribution of a broad-band emission of  $\text{Ce}^{3+}$  ions located in the blue region of the electromagnetic spectrum, a well-defined green emission of  $\text{Tb}^{3+}$  ions with the main peak located at  $\lambda_{\text{Em}} = 545$  nm in the YSO phosphor, and a broad-band emission in the red region due to  $\text{Eu}^{2+}$  ions in the SSN phosphor. It is worth mentioning that excitation wavelength was in long UV radiation at 360 nm. In addition, a predictive model simulating and modelling the rare earths' molar percentages to approximate to the D65 white light chromaticity coordinates is presented.

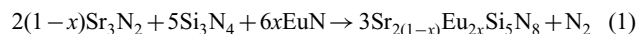
**1. Introduction:** Nowadays generation of white-light emitting solid-state sources is a research area of great importance. Light-emitting diodes (LEDs) are considered the next generation source of light and general lighting. Also, development of white light approaches has had a breakthrough due to the progression of gallium nitride-based semiconductor technology. On the other hand, current conditions in the biological sciences reflect the need for developing new phosphor materials that meet LEDs requirements to develop white-light solid-state sources, among many other applications [1–4].

Research has shown that  $\text{Y}_2\text{SiO}_5\text{:Ce, Tb}$  phosphor ( $\text{YSO:Ce, Tb}$ ) emits white-light due to simultaneous  $\text{Ce}^{3+}$  and  $\text{Tb}^{3+}$  emissions in the blue region of electromagnetic spectrum and a well-defined peak around 546 nm wavelength, respectively [5, 6]. However,  $\text{YSO:Ce, Tb}$  needs a red emission contribution to improve white light and achieve D65 chromaticity coordinates. In this sense, many studies on luminescent properties of  $\text{Eu}^{2+}$  in different host lattice materials have reported that emission from  $\text{Eu}^{2+}$  ions exhibits two types of transitions, among which  $4f^65d \rightarrow 4f^7$  ( $^8\text{S}_{7/2}$ ) transition is the most common. Such  $\text{Eu}^{2+}$  ions emission can be extended in a broader range from ultra-violet to red region of the visible spectrum, depending of host lattice where  $\text{Eu}^{2+}$  is incorporated [7].

Based on the above, we considered that  $\text{YSO:Ce, Tb}$  has excellent properties which can be met with  $\text{Sr}_2\text{Si}_5\text{N}_8\text{:Eu}^{2+}$  phosphors (SSN:Eu). This red-emitting phosphor has a broad emission band, and its most important property is its very broad excitation band from 250 to 500 nm wavelengths [8]. Thus, SSN:Eu can absorb the same excitation wavelength of  $\text{YSO:Ce, Tb}$  (360 nm), thereby implying that with only one excitation wavelength we can activate both phosphors  $\text{YSO:Ce, Tb}$  and  $\text{SSN:Eu}$  to produce a trichromatic source of white-light emission with D65 light chromaticity coordinates.

**2. Methodology:** We synthesised  $\text{Y}_2\text{SiO}_5\text{:Ce, Tb}$  phosphor material using the pressure-assisted combustion method, thoroughly described in a previous work [5]. Molar percentages were 0.75% for  $\text{Ce}^{3+}$  ions, whereas  $\text{Tb}^{3+}$  ions varied from 1.00 to 6.00 to achieve D65 white light. Also, we synthesised  $\text{Sr}_2\text{Si}_5\text{N}_8\text{:Eu}^{2+}$  through a solid-state reaction from  $\text{Sr}_3\text{N}_2$ ,  $\text{EuN}$ ,  $\text{Si}_3\text{N}_4$  as reagents [8].  $\text{Sr}_3\text{N}_2$  and  $\text{EuN}$  were prepared from pure strontium

and europium metals, and both metals were subject to a nitriding process under  $\text{N}_2$  flow at 800°C for 12 h. Obtained substances were black pieces in both cases. Likewise, we weighted reagents  $\text{Sr}_3\text{N}_2$ ,  $\text{EuN}$ , and  $\text{Si}_3\text{N}_4$  (Alfa-Aesar) according the following chemical reaction



All reagents were blended and ground together in an agate mortar into a glove box under  $\text{N}_2$  atmosphere. The resulting blend was transferred into molybdenum boats. Immediately, boats with powder blends were subject to an annealing treatment at 1400°C for 14 h in a horizontal tube furnace under flowing 90%  $\text{N}_2$  and 10%  $\text{H}_2$  atmosphere. Once the temperature was below 60°C, the product was removed from the horizontal tube furnace. We obtained orange to red powders as  $\text{Sr}_2\text{Si}_5\text{N}_8\text{:Eu}$  products, with increasing  $\text{Eu}^{2+}$  ions molar percentages. The  $\text{Eu}^{2+}$  ions molar percentages varied from 5 to 100% in the  $\text{SSN:Eu}^{2+}$  phosphor series.

**3. Experimental data:** We determined the crystallographic structure of particles through X-ray diffraction (XRD, PHILIPS X' Pert) using  $\text{Cu-K}\alpha$  radiation. The crystalline structure of synthesised  $\text{Sr}_2\text{Si}_5\text{N}_8\text{:Eu}^{2+}$  phosphors showed an orthorhombic lattice with the space group of  $\text{Pmn}2_1$ . Then, crystalline structures were associated to JCPDS Card Nos. 85-0101 and 87-0423, for low and high  $\text{Eu}^{2+}$  molar percentages. These cards match  $\text{Sr}_2\text{Si}_5\text{N}_8$  and  $\text{Eu}_2\text{Si}_5\text{N}_8$  crystalline structures, respectively. Also, we replaced strontium ions with  $\text{Eu}^{2+}$  ions, since both  $\text{Sr}_2\text{Si}_5\text{N}_8$  and  $\text{Eu}_2\text{Si}_5\text{N}_8$  are isostructural compounds [8]. As result, diffraction patterns (Fig. 1) for low and high  $\text{Eu}^{2+}$  molar percentages showed the same  $2\theta$ -peak positions, showing only small variations in peak intensities.

We obtained morphology images and particles size of resulting powders through transmission electron microscopy (TEM, JEOL 2010). Shape and particles size are shown in Fig. 2. These particles presented irregular shape and sizes from 200 nm to bigger and formed agglomerations.

Luminescent properties of all phosphor materials reported in this Letter were performed by photoluminescence using a fluorescence

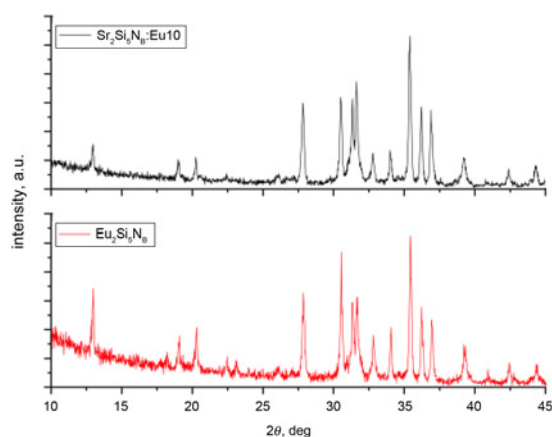


**Fig. 1** XRD patterns of 10%  $\text{Eu}^{2+}$  doped  $\text{Sr}_2\text{Si}_5\text{N}_8$  and  $\text{Eu}_2\text{Si}_5\text{N}_8$  phosphors

spectrophotometer (PL, HITACHI f-7000 fluorescence spectrophotometer). In the case of excitation spectra, the maximum excitation wavelength was around 360 nm, and this single excitation wavelength was enough to activate emission of both Ce and Tb ions, due to the energy transfer process from Ce ions to Tb ions. Then, emission spectra consisted in simultaneous emission of a blue broadband from Ce ions and a green peak from Tb ions, mainly. Ratio of emission intensities depended on the molar percentage of both rare-earth ions. Properties of this material have been thoroughly studied in previous research [5]. For this work, we use the combinations shown in Table 1.

Fig. 3 shows emission spectra of SSN:Eu<sup>2+</sup> phosphor series for different Eu<sup>2+</sup> ions molar percentages, using 360 nm as excitation wavelength. The broadband emission was due to the  $4f^65d^1 \rightarrow 4f^7$  transition of Eu<sup>2+</sup> ions. These emission spectra show a red shift in the maximum emission wavelength, with increasing Eu<sup>2+</sup> ions associated with the nephelauxetic effect and crystalline field, according to other reports [4, 9–11]. In addition, it can be observed a luminescence intensity decrease with the Eu<sup>2+</sup> ions molar percentages increase. Also, Fig. 3 shows excitation spectra for different Eu<sup>2+</sup> ions molar percentages. Excitation spectra consist in a very broad band, from 250 to 550 nm wavelengths, with maximum absorptions in 250, 310, 385, and 448 nm. The 250 nm wavelength absorption is usually associated with host absorption, whereas the other absorption wavelengths are directly associated with Eu<sup>2+</sup> ions absorption [12].

In order to generate white-light emission with chromaticity coordinates of D65 light, we prepared YSO:Ce, Tb with SSN:Eu blends at different SSN:Eu weight percentages. Since YSO:Ce, Tb has an excitation wavelength of 360 nm, we used 360 nm wavelength to excite YSO:Ce, Tb with SSN:Eu blends. Fig. 4 shows emission spectra of YSO:Ce, Tb with SSN:Eu blends at different SSN:Eu weight percentages. The excitation wavelength was 360 nm only, meaning that both phosphor materials, YSO and SSN, absorbed the same excitation wavelength, and even SSN absorbed blue and green emissions from YSO:Ce, Tb phosphors.

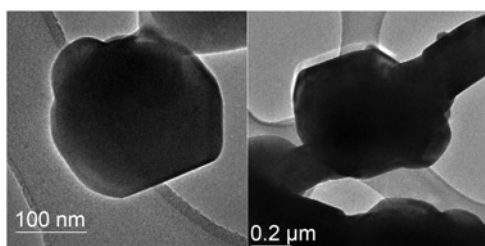


**Fig. 2** TEM images of SSN:Eu particles

**Table 1** Phosphor materials combinations

Blend name	Ce, molar %	Tb, molar %	Eu, molar %	SSN, mass %
Blend01	0.75	2.8	10	1
Blend02	0.75	2.8	20	1
Blend03	0.75	3.35	5	1
Blend04	0.75	3.35	5	1
Blend05	0.75	3.35	5	2
Blend06	0.75	3.35	10	1
Blend07	0.75	3.35	10	2
Blend08	0.75	3.35	20	1.5
Blend09	0.75	3.35	20	2
Blend10	0.75	4	5	1
Blend11	0.75	4	10	1
Blend12	0.75	5	10	1
Blend13	0.75	6	10	1

Obtained emission spectra consisted in six emission signals, a violet-blue broadband in the range from 375 to 450 nm, produced by Ce<sup>3+</sup> ions; four peaks centred in 488, 546, 585, and 624 nm originated from Tb<sup>3+</sup> ions; and a red broadband in the range from 600 to 750 nm, originated from Eu<sup>2+</sup> ions. Simultaneous emission from the three rare-earth ions resulted in white-light emission with trend to D65 light. As a result, generated light has potential applications for white-light solid-state lamps. In addition, we observed a decrease in Ce<sup>3+</sup> and Tb<sup>3+</sup> ions emission signals when SSN:Eu phosphors weight percentage increased. This behaviour is due to the fact that SSN:Eu phosphors absorb blue and green emissions from Ce<sup>3+</sup> and Tb<sup>3+</sup> ions, respectively. Also, Fig. 4 shows excitation spectra of YSO:Ce, Tb with SSN:Eu blends. Monitored emission was 415 nm, which fitted the range of Ce<sup>3+</sup> ions emission.

Excitation spectra consisted in three absorption bands with maximums in 241, 301, and 360 nm. The first band was associated with the Tb<sup>3+</sup> ions absorption; the second and third bands were associated with the Ce<sup>3+</sup> ions absorptions. These excitation spectra were similar to YSO:Ce, Tb excitation spectra, since emission corresponded to Ce<sup>3+</sup> ions. Also, note that 360 nm wavelength was the only excitation wavelength used to activate phosphor blends and produce white-light emission.

Fig. 5 shows chromaticity coordinates for YSO:Ce, Tb phosphor series (blue diamonds), SSN:Eu phosphor series (green triangles), and YSO:Ce, Tb-SSN:Eu blends (rest of graphics points). In the YSO:Ce, Tb phosphor series, molar percentage of Ce<sup>3+</sup> was kept in 0.75, whereas Tb<sup>3+</sup> varied from 1.00 to 6.00, in substitution of Y<sup>3+</sup>, for both rare-earth ions. In the case of SSN:Eu phosphor

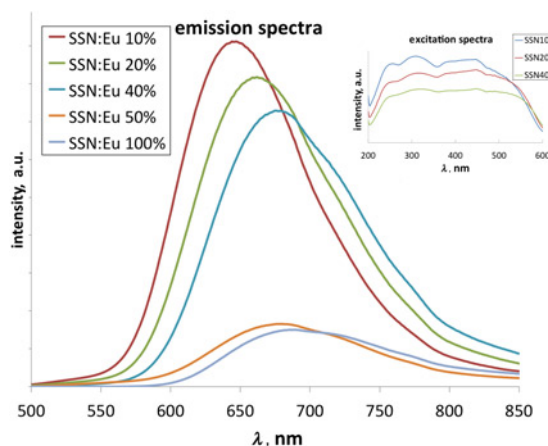


**Fig. 3** Emission and excitation spectra for different  $\text{Eu}^{2+}$  molar percentages in the SSN:Eu<sup>2+</sup> phosphors

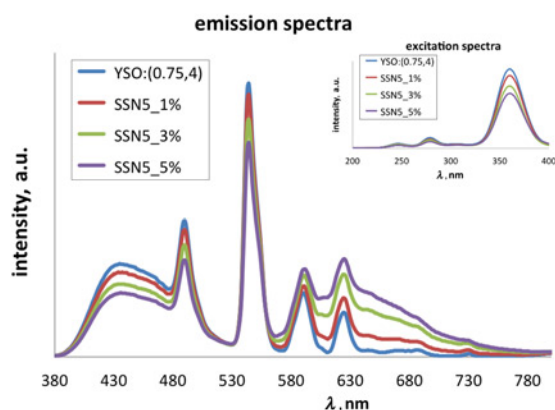


**Fig. 4** Emission and excitation spectra of YSO:Ce<sup>3+</sup>, Tb<sup>3+</sup> with SSN:Eu<sup>2+</sup> phosphors blends using 360 nm as excitation wavelength only

series, molar percentage of Eu<sup>2+</sup> ions varied from 5 to 100 in substitution of Sr<sup>2+</sup>. It is possible to obtain different YSO:Ce, Tb with SSN:Eu combinations to produce light with trend to D65 light from this trichromatic source; it depends on the rare-earth ions molar percentages used to synthesise YSO:Ce, Tb and SSN:Eu phosphors.

We obtained the best white light approach – chromaticity coordinates (0.3172, 0.3262) – using rare-earth ions molar percentages of 0.75 and 4% for Ce<sup>3+</sup> and Tb<sup>3+</sup>, respectively, in the YSO:Ce, Tb phosphor material, and 5% for Eu<sup>2+</sup> in the SSN:Eu phosphor material. Similarly, phosphor material blend weigh percentage was 97 and 3% for YSO:Ce, Tb and SSN:Eu, respectively. A white-light trichromatic approach from Eu<sup>2+</sup> doped Sr<sub>2</sub>Si<sub>5</sub>N<sub>8</sub> and YAG:Ce, combined with blue emitting LED, has been reported in research conducted by Brinkley *et al.* [2], his approach resulting in  $x = 0.39474$  and  $y = 0.39738$  chromaticity coordinates.

**4. Predictive model:** We propose a simulation model as shown in Fig. 6, which used data presented in Table 2. As can be observed, we obtained chromaticity coordinates for each emission spectra and used them to calculate Euclidean distance (ED) and Mahalanobis distance (MD). After calculating MD, we built a model to

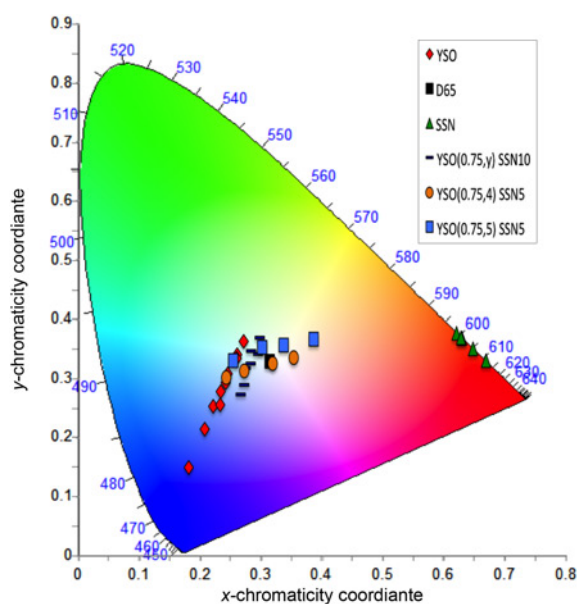


**Fig. 5** Chromaticity coordinates of YSO:Ce,Tb (diamonds), SSN:Eu (triangles) before blending, YSO:Ce, Tb-SSN:Eu blends (circles, squares, and dashes), and D65 white light (black square)

approximate to the white light coordinates, according to CIE1931 (D65), which are (0.3128, 0.329), and experimental data.

A wide range of distance measures is used in science to reduce problem dimensions, thereby simplifying the number of variables and enabling to obtain simple geometric representations of data. In this sense, although the ED is one of the most used, it is not enough for studies when variables are correlated, as it is the case of this research. For this reason, we relied on the MD, which takes into account covariance matrix between data [13]. Also, the MD decreases as correlation between variables increases, and it is calculated with the following equation

$$MD(x) = \sqrt{(x - \mu)^T S^{-1} (x - \mu)} \quad (2)$$

where  $x$  represents random variables with covariance matrix  $S$ . In this case,  $x$  are chromaticity coordinates values. Table 2 shows ED and MD results.

Also, as regression method, we followed a linear least square approach, and its high-level algorithm is as follows [14, 15].

**Algorithm 1:** Regression with linear least square

Input: A set of  $m$  linear equations, each one with  $n$  independent variables and one dependent variable, given by the previous set of experimental results.

Step 1. State each input equation as:  $f(x, \beta) = \beta_0 + \beta_1 x_1 + \dots + \beta_n x_n$ . Where each independent variable ( $x_1, x_2, \dots, x_n$ ) represents the molar percentage of rare earths, and the estimated  $f(x, \beta)$  values are given by results of the input experiments.

Step 2. Use quadratic minimisation to find the coefficients  $\beta_0, \beta_1 x_1, \dots, \beta_n x_n$ , setting the system in matrix equation of the type  $Ax = b$  with the formula:  $(A^T A)\beta = A^T y$ .

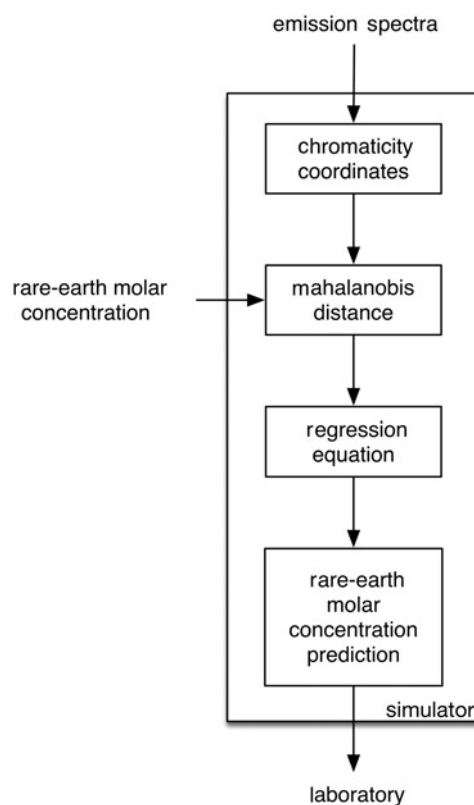


**Fig. 6** Proposed methodology using Mahalanobis distance

**Table 2** Chromaticity coordinates and distance values

Blend name	<i>x</i> (CIE 1931)	<i>y</i> (CIE 1931)	<i>ED</i>	<i>MD</i>
Blend01	0.2646	0.2728	0.0740	3.490
Blend02	0.2704	0.2714	0.0715	3.148
Blend03	0.2642	0.294	0.059	3.470
Blend04	0.2692	0.2969	0.054	3.111
Blend05	0.2946	0.3069	0.028	1.325
Blend06	0.2706	0.2894	0.057	3.009
Blend07	0.3016	0.3014	0.029	1.090
Blend08	0.2869	0.2958	0.042	1.901
Blend09	0.3013	0.3032	0.028	1.051
Blend10	0.2703	0.3137	0.045	3.142
Blend11	0.2728	0.3179	0.041	2.997
Blend12	0.2819	0.3465	0.035	2.835
Blend13	0.2959	0.3697	0.044	2.554

*ED*: Euclidean distance, *MD*: Mahalanobis distance

Step 3. Calculate from previous formula the estimated slope and coefficients for independent variables and report them as output.

This algorithm gave as results a set of coefficients, as shown in the following equation.

$$MahaDist = 6.23 - 0.246Tb - 0.0204Eu - 2.02 \text{ mass} \quad (3)$$

which give us a value of  $R^2 = 98.4\%$ .

Given the previous equation, we conducted a search for blends closer to white light based on the regression. We used Algorithm 2 to search for a set of blend components combination following the bisection method [16].

**Algorithm 2:** Bisection search for rare-earth's components

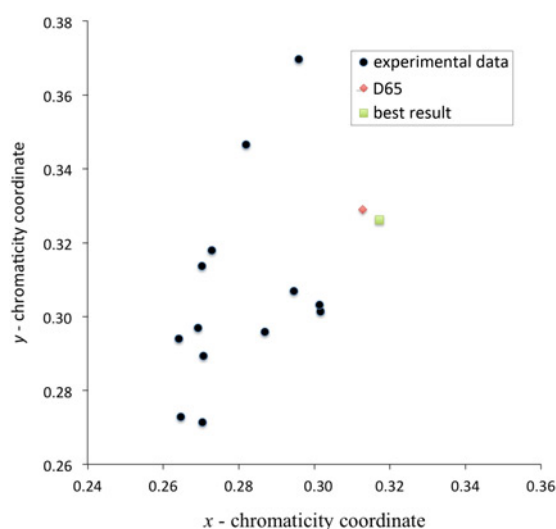
Input: A set of values ( $x_1, x_2, \dots, x_n$ ), each one representing the molar percentage of rare earths and the SSN:Eu mass percentage for nearest-to-white-light known experimental result. A set of values ( $\delta_1, \delta_2, \dots, \delta_n$ ) representing the maximum difference between experimental values for each parameter ( $x_i$ , where  $i \in [1 \dots n]$ ). A set of weights ( $w_1, w_2, \dots, w_n$ ) representing the relative weights according to their market prices.

Step 1. For each variable  $x_i$ , where  $i \in [1 \dots n]$ , calculate a new value from (3), with a value  $MahaDist = 0$ , using a modified Bisection Method as follows:

**Table 3** Combinations suggested by Bisection searching algorithm

Blend name	Tb, molar %	Eu, molar %	SSN, mass %	<i>MD</i>
Blend09	3.350	20.000	2.000	10.514
Pred01	3.3505	15.000	2.524	8.377
Pred02	2.8005	15.000	2.591	8.143
<b>Pred03</b>	<b>3.899</b>	<b>10.820</b>	<b>2.500</b>	<b>6.776</b>
Pred04	3.3495	17.452	2.500	9.452
Pred05	2.8000	20.000	2.541	10.337
Pred06	2.8000	15.000	2.591	8.143
Pred07	3.1382	20.000	2.500	10.481
Pred08	3.5528	15.000	2.500	8.463
<b>Pred09</b>	<b>3.900</b>	<b>10.910</b>	<b>2.499</b>	<b>6.816</b>
Pred10	3.9000	60.420	1.999	28.540
Pred11	3.5609	15.000	2.499	8.466
Pred12	7.6666	15.000	1.999	10.213

*MD*: Mahalanobis distance

**Fig. 7** Best result to produce white light (D65) after prediction with  $Tb = 3.9\%$ ,  $Eu = 10.9\%$ , and mass of SSN = 2.5% (green square)

Step 2. Calculate the high point as  $hp = x_i + \delta_i$  and low point as  $lp = x_i - \delta_i$ . Add hp and lp to solution set.

Step 3. Select the range to apply bisection method by comparing combinations between hp and lp and for each variable pair ( $x_j, x_i$ ) such that  $j \neq i$  and  $i, j \in [1 \dots n]$ .

Step 4. Apply bisection method, searching for the lowest total price, according to relative weights, until the stopping criterion is reached. Add combination found to solution set and go to Step 1.

Step 5. Report solution set as output.

**5. Results:** Table 3 shows the suggested combination after applying Algorithm 2 with Blend09 as starting point, and  $\delta$ -values 0.5, 5, and 0.5 for Tb, Eu, and SSN, respectively. As can be observed, the best combinations (Pred03 and Pred09, in bold) followed the same tendency: to increase Tb and SSN, while decreasing Eu. Such tendency was validated in the laboratory by experts in nanomaterials development, reaching the best result with values 0.75, 4, 5, and 3 for Ce, Tb, Eu, and SSN, respectively, obtaining a better result with a *ED* of 0.005, as shown in Fig. 7.

However, given the applications of this type of materials it is necessary to carry out measurements at different temperatures to ensure the thermal stability of the applications. In this work, the results presented were carried out with experimental measurements at room temperature, additionally measurements were made at low temperature of liquid nitrogen in which a change in the relationship of intensities between the peaks of the different rare earths was observed. The variations observed in the case of the maximum ratios of Ce with respect to Tb are presented in Table 4, where Ce and Tb energy transfer is carried out and could be affected by

**Table 4** Relative intensity for different set of experiments

Blend number	Tb, molar %	Eu, molar %	SSN, mass %	Relative intensity, %
1	4	5	1	15
2	4	5	3	13
3	5	5	1	2
4	5	5	3	4
5	5	5	5	0

temperature variations [17, 18]; in this table it can be seen that the values in the set of experiments where the combinations of Ce = 0.75%, Tb = 5%, Eu = 5% and the mass of SSN from 1 to 5%, are in the range of 0 to 4%.

**6. Conclusions:** Simultaneous emission of cerium and terbium activated yttrium silicate phosphor and europium activated strontium silicon nitride phosphor produces white light with chromaticity coordinates of D65 reference. In this study, we developed a model to predict molar percentage of rare-earth cerium and terbium in the yttrium silicate host and molar percentage of europium in the strontium silicon nitride host. Also, we created the SSN:Eu mass percentage to reach D65 white light chromaticity coordinates and decrease the number of experiments in the laboratory with a correlation value  $R^2 = 98.4\%$ . In addition, we developed the graphical interface in NetLogo, which helped jointly display the emission spectra and chromaticity coordinates of experimental data. The graphical interface produced a list of molar concentrations of rare earths and mass percentage of strontium silicon nitride that binds the set of experiments performed in the laboratory.

**7. Acknowledgment:** This work was partially supported by Universidad Autónoma de Baja California and Centro de Nanociencias y Nanotecnología.

## 8 References

- [1] Sokolnicki J.: 'Rare earths (Ce, Eu, Tb) doped  $Y_2Si_2O_7$  phosphors for white LED', *J. Lumin.*, 2013, **134**, pp. 600–606. Available at <http://dx.doi.org/10.1016/j.jlumin.2012.07.023>
- [2] Brinkley S.E., Pfaff N., Denault K.A., *ET AL.*: 'Robust thermal performance of  $Sr_2Si_5N_8:Eu^{2+}$ : An efficient red emitting phosphor for light emitting diode based white lighting', *Appl. Phys. Lett.*, 2011, **99**, pp. 241106-1–241106-3. Available at <http://dx.doi.org/10.1063/1.3666785>
- [3] Ima W.B., Yoo H.S., Vaidyanathan S., *ET AL.*: 'A novel blue-emitting silica-coated  $KBaPO_4:Eu^{2+}$  phosphor under vacuum ultraviolet and ultraviolet excitation', *Mater. Chem. Phys.*, 2009, **115**, pp. 161–164. Available at <http://dx.doi.org/10.1063/1.3666785>
- [4] Xie R.-J., Hirosaki N., Sakuma K., *ET AL.*: 'White light-emitting diodes (LEDs) using (oxy)nitride phosphors', *J. Phys. D Appl. Phys.*, 2008, **41**, pp. 144013-1–144013-5
- [5] Cervantes-Vásquez D., Contreras O.E., Hirata G.A.: 'Quantum efficiency of silica-coated rare-earth doped yttrium silicate', *J. Lumin.*, 2013, **143**, pp. 226–232
- [6] Cervantes D., Flores D.L., Gutierrez E., *ET AL.*: 'Ce, Tb-Doped  $Y_2SiO_5$  phosphor luminescence emissions modeling and simulation', *Adv. Struct. Mater.*, 2016, **33**, pp. 145–156
- [7] Kohale R.L., Dhoble S.J.: 'Luminescence in Eu21-activated micro-crystalline pyrophosphor', *Micro Nano Lett.*, 2012, **7**, (5), pp. 453–455. Available at 10.1049/mnl.2012.0173
- [8] Li Y.Q., van Steen J.E.J., Krevel J.W.H., *ET AL.*: 'Luminescence properties of red-emitting  $M_2Si_5N_8:Eu^{2+}$  (M=Ca, Sr, Ba) LED conversion phosphors', *J. Alloys Comp.*, 2006, **417**, pp. 273–279
- [9] Duan C.J., Otten W.M., Delsing A.C.A., *ET AL.*: 'Preparation and photoluminescence properties of  $Mn^{2+}$ -activated  $M_2Si_5N_8$  (M=Ca, Sr, Ba) phosphors', *J. Solid State Chem.*, 2008, **181**, pp. 751–757
- [10] Xiaoming T., Weidong Z., Yunsheng H., *ET AL.*: 'Luminescence properties of nitride red phosphor for LED', *J. Rare Earth*, 2008, **26**, (5), pp. 652–655
- [11] Song X., Fu R., Agathopoulos S., *ET AL.*: 'Luminescence and energy transfer of  $Mn^{2+}$  co-doped  $SrSi_2O_2N_2:Eu^{2+}$  green-emitting phosphors', *Mater. Sci. Eng. B*, 2009, **164**, pp. 12–15
- [12] Piao X., Horikawa T., Hanzawa H., *ET AL.*: 'Characterization and luminescence properties of  $Sr_2Si_5N_8:Eu^{2+}$  phosphor for white light-emitting-diode illumination', *Appl. Phys. Lett.*, 2006, **88**, pp. 161908-1–161908-3
- [13] Mahalanobis P.C.: 'On the generalized distance in statistics', *Proc. Natl. Inst. Sci. India A, Phys. Sci.*, 1936, **2**, (1), pp. 49–55
- [14] Lawson C.L., Hanson R.J.: 'Solving least squares problems' (Prentice-Hall, Englewood Cliffs, NJ, 1974), ISBN 0-13-822585-0
- [15] NIST/SEMATECH: 'e-Handbook of statistical methods'. Available at <http://www.itl.nist.gov/div898/handbook/>, visited October 2016
- [16] Burden R.L., Faires J.D.: '2.1 The Bisection algorithm', 'Numerical analysis' (PWS Publishers, 1985, 3rd edn.), ISBN 0-87150-857-5
- [17] Zhang X., Zhou L., Pang Q., *ET AL.*: 'A broadband-excited and narrow-line  $GdBO_3:Ce^{3+}, Tb^{3+}, Eu^{3+}$  red phosphor with efficient  $Ce^{3+} \rightarrow (Tb^{3+})n \rightarrow Eu^{3+}$  energy transfer for NUV LEDs', *Opt. Mater.*, 2014, **36**, (7), pp. 1112–1118. Available at 10.1016/j.optmat.2014.02.009
- [18] Tian Y.: 'Development of phosphors with high thermal stability and efficiency for phosphor-converted LEDs', *J. Solid State Light.*, 2014, **1**, pp. 1–11. Available at 10.1186/s40539-014-0011-8